Full Paper

Propellants, Explosives, Pyrotechnics

DOI: 10.1002/prep.201400112

Effects of MgH_2/$Mg(BH_4)_2$ Powders on the Thermal Decomposition Behaviors of 2,4,6-Trinitrotoluene (TNT)

Miao Yao,[a] Liping Chen,*[a] and Jinhua Peng[a]

Abstract: The thermal properties of 2,4,6-trinitrotoluene (TNT), TNT/MgH_2, and TNT/$Mg(BH_4)_2$ were investigated by differential scanning calorimetry (DSC) and accelerating rate calorimetry (ARC). The results show that addition of MgH_2 or $Mg(BH_4)_2$ to TNT has a great effect on the DSC decomposition process. The exothermic decomposition peak of TNT disappeared and was replaced by a slow exothermic trend in the curves of both TNT/MgH_2 and TNT/$Mg(BH_4)_2$. The kinetic triplet of TNT formulations were calculated by ARC data. The results show that TNT/MgH_2 and TNT/$Mg(BH_4)_2$ have lower onset temperatures, apparent activation energies (*E*) and frequency factors (*A*) than neat TNT. A change of the TNT decomposition mechanism is also discussed.

Keywords: Differential scanning calorimetry · Magnesium · Trinitrotoluene · Decomposition · Thermal properties

1 Introduction

After aluminum powder has been commonly applied [1–4], metal hydrides are used in explosives, propellants, and pyrotechnic compositions in order to improve the detonation performance of energetic materials. The most important reason is that hydrogen stored in metal hydrides is expected to provide more energy as fuel. Magnesium has the largest hydrogen storage capacity among all metals of up to 7.6 wt-% in MgH_2. $Mg(BH_4)_2$ is another magnesium-based complex hydride, which contains 14.9 wt-% hydrogen. Their high hydrogen storage capacities make these compounds promising candidates for explosive formulations.

Kwok and Jones et al. investigated the effects of different sized Al powders on the thermal stability of TNT, RDX, Composition B, and AP by accelerating rate calorimetry (ARC) [5,6]. Liang et al. studied the effect of nano-sized Al powder on catalytic performance of the thermal decomposition of HMX and RDX [7]. Liu et al. synthesized MgH_2, Mg_2NH_4, Mg_2Cu-H and investigated the thermal properties of their mixtures with AP by differential scanning calorimetry (DSC) [8,9].

In this study, MgH_2 and $Mg(BH_4)_2$ powders were mixed with TNT in order to study their effects on the thermal decomposition of TNT. DSC and ARC were used to investigate the thermal and kinetic properties of TNT formulations. In addition, the effect of these metal hydrides on the decomposition mechanism of TNT was analyzed.

2 Experiment

2.1 Materials

MgH_2 and $Mg(BH_4)_2$ powders were obtained from Shanghai Engineering Research Center of Magnesium Materials and Application. MgH_2 was prepared by a DC Arc Plasma method followed by hydrogenation under high pressure [10]. $Mg(BH_4)_2$ was synthesized by a wet chemical method [11,12]. Both hydrides reach the μm size. TNT was dried at 60 °C to constant mass before use. TNT and the metal hydrides were manually mixed at different ratios. The results for mixtures of 90 : 10 mass ratios are presented herein.

2.2 DSC and ARC

A DSC apparatus by Mettler Toledo (model: DSC1) was used in this study. About 1 mg of MgH_2/$Mg(BH_4)_2$ powders and their mixtures with TNT were tested at 10 °C min^{-1} in the temperature range 25–500 °C in a 30 mL min^{-1} nitrogen flow. A 30 μL stainless steel crucible was used.

Compared with DSC, ARC has a larger sample quantity and is run under adiabatic conditions. A lightweight spherical titanium bomb was used in this experiment. A Thermal Hazard Technology (model: esARC) instrument was used. The ARC experiments started at atmospheric pressure, a temperature of 20 °C, and a relative humidity of 30 %, and afterwards continued in a closed configuration. The standard ARC procedure of heat-wait-search was used.

[a] *M. Yao, L. Chen, J. Peng*
School of Chemical Engineering
Nanjing University of Science & Technology
Nanjing, Jiangsu 210094, P. R. China
**e-mail: clp2005@hotmail.com*

Table 1. Hydrogen releasing temperature of MgH_2.

Ref.	T_p [°C]	Test condition	Sample
[13]	430 [a]	PDSC, 5 °C min^{-1} heating rate, 0.2 MPa of hydrogen	The average particle size was 20 μm. (95 wt-% MgH_2, 5 wt-% Mg)
[13]	366 [a]	PDSC, 5 °C min^{-1} heating rate, 0.2 MPa of hydrogen	20 h milled 20 μm magnesium hydride by a Spex 8000 model shaker mill
[14]	363 [a]	DSC-MS, 50 mL min^{-1} argon flow	Ball-milled commercial MgH_2 (Alfa Aesar, 98 wt-% MgH_2)
[15]	287 [b]	Pressure-tight vessel under isothermal	Commercial MgH_2 (7.5 wt-% Mg, 3.7 wt-% MgO)

a) Peak temperature. b) Initial temperature.

Table 2. Hydrogen releasing temperature of $Mg(BH_4)_2$.

Ref.	T_p [°C]	Test condition	Sample
[16]	301, 372 [a]	TG-DTA, 5 °C min^{-1} heating rate, 150 mL min^{-1} He flow	β-$Mg(BH_4)_2$ was synthesized by metathesis reaction of $MgCl_2$ with $NaBH_4$ in diethyl ether and crystallized out at a high temperature
[17]	290 [a]	HP-DSC, 10 °C min^{-1} heating rate, 50 mL min^{-1} He flow or 0.5 MPa H_2	α-$Mg(BH_4)_2$ was synthesized by reaction of $MgCl_2$ with $NaBH_4$ in diethyl ether and crystallized out at a low temperature
[18]	167 [a]	DSC, 5 °C min^{-1} heating rate at 10 MPa of hydrogen	Synthesized by reaction of $MgCl_2$ with $LiBH_4$

a) Peak temperature.

3 Results and Discussion

3.1 Thermal Behaviors of MgH_2 and $Mg(BH_4)_2$

The kinetic properties of dehydriding and rehydriding of hydrogen storage materials have been intensively studied. Some literature data on the hydrogen release temperatures of MgH_2 and $Mg(BH_4)_2$ are collected in Table 1 and Table 2. According to the literature, hydrogen release is an endothermic process, but the literature data for hydrogen release temperatures are quite different. This difference may be caused by different preparation methods and test conditions. MgH_2 and $Mg(BH_4)_2$ have relatively high hydrogen release temperatures and don't seem to be well-suited as hydrogen storage materials. A high hydrogen release temperature, however, proves to be beneficial for an explosive component due to the reasonably good thermal stability. The thermal behaviors of MgH_2 and $Mg(BH_4)_2$ powders were investigated by DSC and the results are shown in Figure 1.

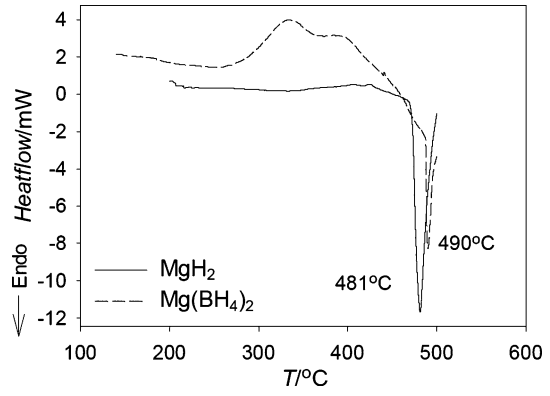

Figure 1. DSC results of MgH_2 and $Mg(BH_4)_2$ in N_2 at 10 °C min^{-1}.

It can be seen that MgH_2 has an endothermic peak at 481 °C. The endothermic peak of $Mg(BH_4)_2$ is at 490 °C after a broad exothermic reaction. It was reported that $Mg(BH_4)_2$ decomposes to intermediate compounds, thereby desorbing a small amount hydrogen and the endothermic peak is actually the decomposition of MgH_2. Hydrogen releasing of $Mg(BH_4)_2$ thus might start from 260 °C onwards.

3.2 Thermal Behaviors of TNT and Mixtures of TNT with MgH_2/$Mg(BH_4)_2$ Powders

DSC results for TNT formulations are shown in Figure 2 and Table 3. It can be seen that TNT melted at about 80 °C and decomposed at about 300 °C. By addition of 10% of MgH_2 the exothermic decomposition peak disappeared and was replaced by a slow and broad exothermic signal. The same phenomenon occurred when 10% of $Mg(BH_4)_2$ was added. The TNT/10%$Mg(BH_4)_2$ mixture had a slightly lower onset temperature than the TNT/10%MgH_2 mixture. Besides, mixtures with other proportions (TNT/5% metal hydride and TNT/2% metal hydride) were also tested and similar results were obtained. The reason for this effect is discussed Section 3.3. It is shown in Figure 2 that an endotherm appears at around 460 °C in the DSC curve of TNT/MgH_2. The presence of this peak indicated that there was still some MgH_2 left in the crucible. The grey baselines in Figure 2 were chosen to estimate the heat releases of the mixtures and

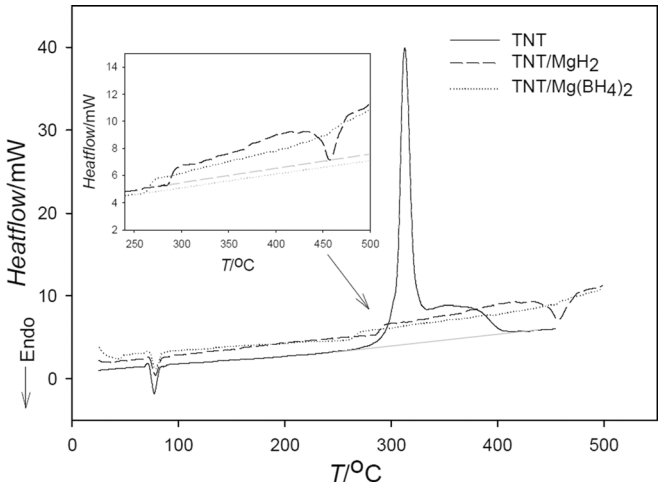

Figure 2. DSC results of TNT formulations in N_2 at 10 °C min^{-1}.

Table 3. DSC results for different TNT formulations.

Sample	*M* [mg]	T_0 [°C]	*Q* [mJ]	*Q** [J g^{-1}]
TNT	1.05	303.7	4413	4203
TNT/MgH_2	1.06	287.3	2541	2663
TNT/$Mg(BH_4)_2$	1.07	263.9	3401	3532

Table 4. ARC results for different TNT formulations.

Sample	*M* [g]	T_0 [°C]	$\triangle T$ [°C]	$\triangle P$ [MPa]	*Q* [J]	*Q** [J g^{-1}]
TNT	0.108	220.8	18.2	0.15	90	836
TNT/MgH_2	0.099	216.0	16.2	0.17	80	813
TNT/$Mg(BH_4)_2$	0.108	216.2	17.2	0.14	86	792

the results are listed in Table 3. Due to the low and wide structure of the heat release of the mixtures, the choice of a suitable baseline has a great influence on the results of the value of energy release. The experiments were stopped at 500 °C, restricted by instrument conditions; the heat generations were thus incomplete. Herein, the grey baselines were fitted to the curves in order to give a rough evaluation.

ARC results of TNT, TNT/10% MgH_2 and TNT/10% $Mg(BH_4)_2$ are shown in Table 4 and Figures 3–7. A 9.157 g titanium alloy bomb was used. The heating step was 3 °C and the waiting time was 10 min. The experimental data show an exotherm of TNT at about 221 °C. The exotherms of TNT/MgH_2 and TNT/$Mg(BH_4)_2$ were detected at about 216 °C. Neat TNT has the highest adiabatic temperature rise ($\triangle T$), maximum self-heating-rate and heat release. TNT/MgH_2 has the highest pressure rise ($\triangle P$), which is reasonable due to the higher temperature for hydrogen release.

Heat release could not be directly obtained from the ARC experiment. The values were calculated from $\triangle T$ and the heat capacities of the samples, and then corrected by thermal inertia as described in the literature [19]. The heat

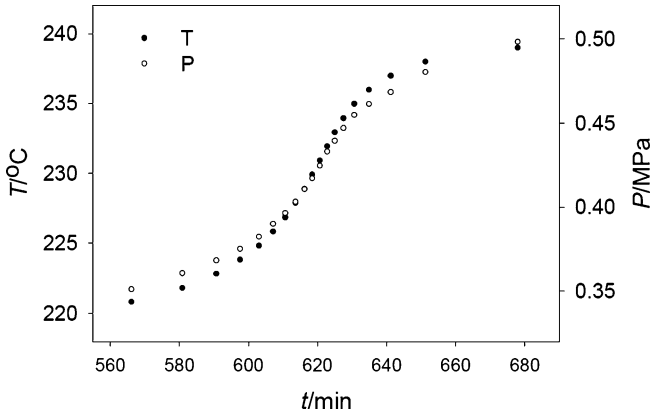

Figure 3. ARC result for TNT (*T* and *P* vs. *t*).

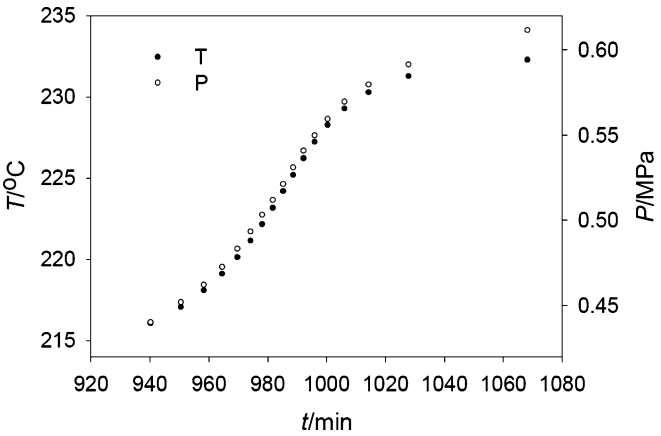

Figure 4. ARC result for TNT/MgH_2 (*T* and *P* vs. *t*).

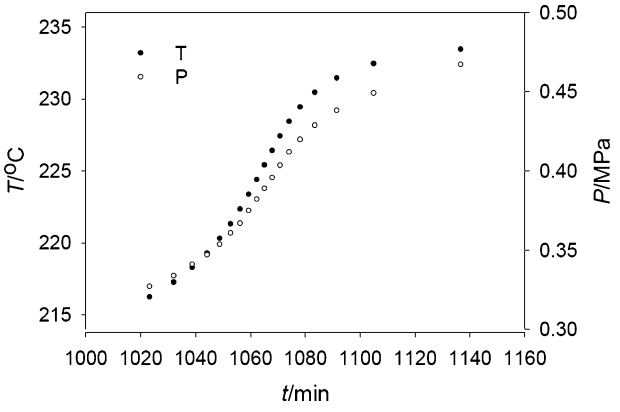

Figure 5. ARC result for TNT/$Mg(BH_4)_2$ (*T* and *P* vs. *t*).

capacities of TNT and bomb are 1.07 and 0.53 J g^{-1} °C, respectively. The Swagelok was not considered as a part of bomb. Due to the small amounts of metal hydrides, the differences in the heat capacities between mixtures and neat TNT were omitted. For a visual comparison, the heats for

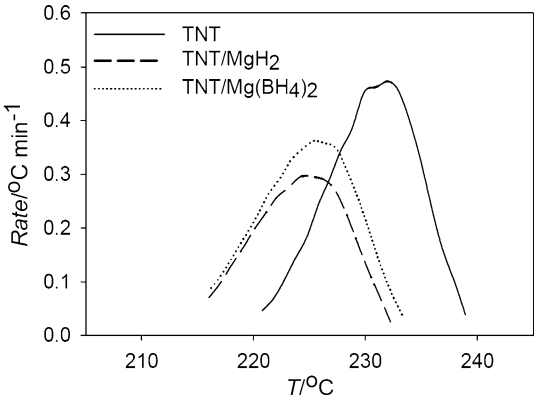

Figure 6. ARC results (*Rate* vs. *T*).

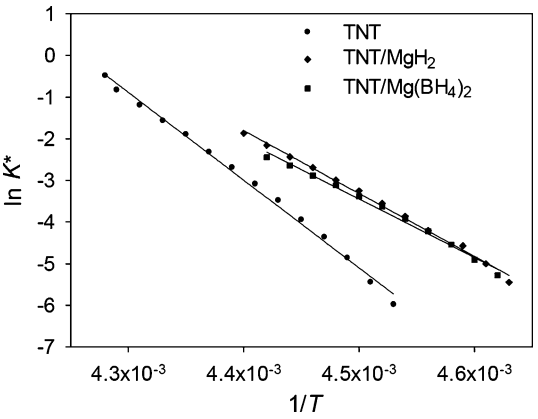

Figure 7. Comparison of ARC results (ln *k** vs. 1/*T*).

TNT (per gram) from DSC and ARC tests were calculated and given as *Q** (Table 3 and Table 4).

The results show large differences between the DSC and the ARC values. The values of *Q** obtained from ARC are much lower than those obtained by DSC, which could be caused by the high thermal inertia. It is well recognized that higher thermal inertia lead to higher onset temperatures and smaller $\triangle T$. The results, however, showed that the addition of two metal hydrides decreased the energy release of TNT.

A pseudo zero-order rate constant is used to calculate the kinetic parameters in this paper [19].

$$\ln k^* = \ln\left(Ac_0^{n-1}\right) - \frac{E}{RT}$$

In Equation (1):

$$k^* = \frac{\mathrm{d}T}{\mathrm{d}t}\left(\frac{\Delta T}{T_\mathrm{f} - T}\right)^n \Delta T^{-1} = Ac_0^{n-1}\exp\left(-\frac{E}{RT}\right)$$

The plots of ln*k** vs. 1/*T* are shown in Figure 7, which is expected to be a straight line when the order of reaction is properly chosen. The Arrhenius kinetic parameters, *E* and *A* were accordingly calculated from the plot.

Table 5. Kinetic parameters of TNT formulations.

Sample	E [kJ mol^{-1}]	lg$A$ [s^{-1}]	n	R^2
TNT	176.6	90.5	2.6	0.99587
TNT/MgH_2	127.2	65.4	1.9	0.99387
TNT/$Mg(BH_4)_2$	112.6	56.9	1.6	0.99337

The kinetic parameters are shown in Table 5. They show that addition of 10% MgH_2 or $Mg(BH_4)_2$ decreased the values of *E* and *A*, which means that both TNT/MgH_2 and TNT/$Mg(BH_4)_2$ have a higher reactivity than TNT. This result agrees with the changes of the onset temperatures in DSC. In addition, $Mg(BH_4)_2$ has higher influence on the thermal stability of TNT than MgH_2.

3.3 Change of Decomposition Mechanism

The thermal decomposition mechanism of TNT was extensively studied. It is believed that at lower temperatures (< 800–900 °C), the initiation chemistry of TNT is dominated by oxidation reactions of the methyl group, while at elevated temperatures (> 800–900 °C), C–NO_2 homolysis dominates the initiation process [20]. The decomposition curves of TNT in DSC and ARC generally follow the process described above. The mechanisms of methyl group oxidations correspond to different sources of oxidant are shown in Scheme 1 and Scheme 2. MgH_2 was prepared through hydrogenation of ultrafine Mg powders, and the high transformation-induced lattice distortion might cause intense cracks in the powder particles. As a result, a number of hydrogen atoms exist in the gaps on the surface of crystal cells [8]. The addition of MgH_2 or $Mg(BH_4)_2$ may introduce reducing hydrogen into the reaction system, which decreases the chance of $-CH_3$ oxidation.

Herein, DSC tests were conducted in an inert nitrogen atmosphere with a small amount of air left in the hermetic crucible. However, in the ARC tests, samples were fully exposed to air. It is calculated that the volume ratios of sample to air are 1:30 and 1:135 in the DSC crucible and the ARC vessel, respectively. Therefore, the $-CH_3$ oxidation in DSC crucible relies more on the nitro groups on the ben-

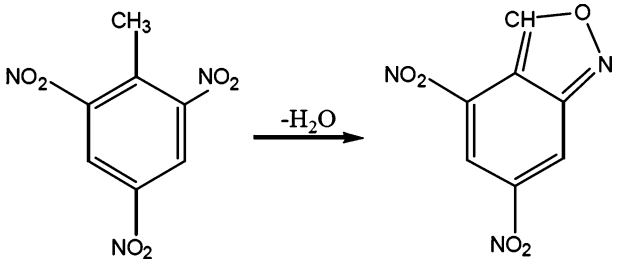

Scheme 1.

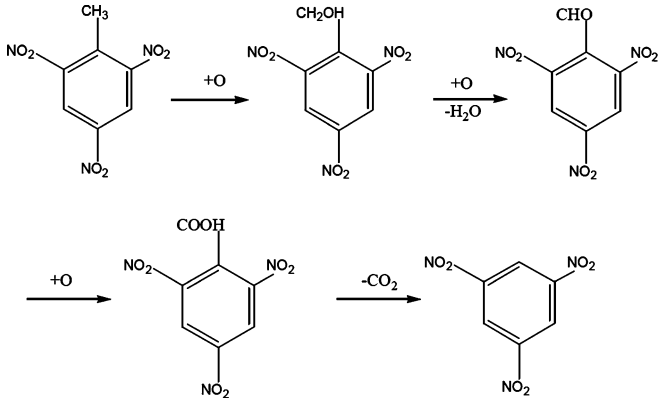

Scheme 2.

zene ring and the introduction of hydrogen has more influence on the decomposition in DSC crucible. On the other hand, the relatively small mass of sample in DSC tests did not favor heat accumulation, and a small amount of magnesium also existed in the products, which helped the heat dissipation. These observations may explain the unusual DSC curves in Figure 2. Furthermore, the existence of MgH_2 or $Mg(BH_4)_2$ could be beneficial to N–O scissions. This may explain why TNT/MgH_2 or TNT/$Mg(BH_4)_2$ has a lower value of *E* and a higher reactivity than neat TNT.

For the detonation process of TNT, the decomposition mechanism appears similar to the one at higher temperature, where C–NO_2 homolysis dominates the initiation process. In this case, the addition of MgH_2 or $Mg(BH_4)_2$ may not have an effect on the –CH_3 oxidation and the detonation process. It was reported that 1–5 % of MgH_2 are sufficient to increase the detonation pressure of TNT [21].

4 Conclusions

The addition of various percentages of MgH_2 or $Mg(BH_4)_2$ powders to TNT significantly affect the DSC decomposition curve of TNT. The exothermic decomposition peak of TNT disappeared and was replaced by a slow and board exothermic trend in both TNT/MgH_2 and TNT/$Mg(BH_4)_2$ curves. The possible reason is that the addition of MgH_2 or $Mg(BH_4)_2$ introduced reducing hydrogen and decreased the chance of –CH_3 oxidation, which is the rate controlling step of TNT decomposition.

The ARC tests show that TNT, TNT/MgH_2 and TNT/$Mg(BH_4)_2$ have similar a heat realizing process. TNT/MgH_2 and TNT/$Mg(BH_4)_2$ have lower onset temperatures and lower values of *E* and *A*. The results imply that the mixtures TNT/MgH_2 and TNT/$Mg(BH_4)_2$ have higher reactivity than neat TNT. In the ARC tests, the samples were exposed to air, which had less effect to the –CH_3 oxidation. In another way, the existence of hydrogen could be helpful to the N–O scissions.

Symbols and Abbreviations

DSC – Differential scanning calorimetry
ARC – Accelerating rate calorimetry
TNT – 2,4,6-Trinitrotoluene
RDX – 1,3,5-Trinitroperhydro-1,3,5-triazine
MgH_2 – Magnesium hydride
$Mg(BH_4)_2$ – Magnesium borohydride
HMX – Octahydro-1,3,5,7-tetranitro-1,3,5,7-tetrazocine
AP – Ammonium perchlorate
PDSC, HP-DSC – Pressure differential scanning calorimetry
MS – Mass spectrometry
TG-DTA – Thermogravimetry and Differential thermal analysis
T_p – Peak temperature [°C]
T_i – Onset temperature [°C]
T_0 – Extrapolated onset temperature [°C]
P – Pressure [MPa]
M – Mass of sample [g]
Q – Heat release value [J]
*Q** – Normalized heat release [J g−1]

Acknowledgments

This research was performed with the help of Professor X. Q. Zeng and Professor J. X. Zou of Shanghai Jiaotong University and Shanghai Engineering Research Center of Magnesium Materials and Application. They are acknowledged for their support.

References

[1] C. B. Roberts, D. D. Toner, *Stabilization of Light Metal Hydride*, US Patent 3,803,082, Dow Chemical Corporation, Midland, MI, USA, **1974**.
[2] J. P. Flynn, G. A. Lane, J. J. Plomer, *Nitrocellulose Propellant Composition Containing Aluminum Hydride*, US Patent 3,844,856, Dow Chemical Corporation, Midland, MI, USA, **1974**.
[3] A. A. Selezenev, V. N. Lashkov, V. N. Lobanov, O. L. Ignatov, A.Yu. Aleinikov, A. V. Strikanov, V. N. Trusov, Effect of Al/AlH_3 and Mg/MgH_2 Components on Detonation Parameters of Mixed Explosives, *12th Symposium on Detonation*, San Diego, CA, USA, 11–16 August, **2002**.
[4] J. R. Ward, *MgH_2 and $Sr(NO_3)_2$ Pyrotechnic Composition*, US Patent 4,302,259, The United States of America as represented by the Secretary of the Army, Washington, D.C, USA, **1981**.
[5] Q. S. M. Kwok, R. C. Fouchard, A. M. Turcotte, P. D. Lightfoot, R. Bowes, D. E. G. Jones, Characterization of Aluminum Nanopowder Compositions, *Propellants Explos. Pyrotech.* **2002**, *27*, 229–240.
[6] D. E. G. Jones, R. Turcotte, R. C. Fouchard, Q. S. M. Kwok, A. M. Turcotte, Z. Abdel-Qader, Hazard Characterization of Aluminum Nanopowder Compositions, *Propellants Explos. Pyrotech.* **2003**, *28*, 120–131.
[7] L. Liang, J. Y. Wang, J. Dong, C. W. An, Effects of Nano-Al powder on the Thermal Decomposition Catalytic Performance of Nitroamine Explosives, *Chin. J. Explos. Propellants* **2009**, *32*, 75–78.

[8] L. L. Liu, F. S. Li, C. L. Zhi, H. C. S, Y. Yang, Q. S. Zhang, Synthesis of Magnesium Hydride and Its Effect on Thermal Decomposition of AP, *Rare Met. Mater. Eng.* **2010**, *39*, 1289–1292.
[9] L. L. Liu, F. S. Li, C. L. Zhi, H. C. Song L. Peng, Effect of Magnesium Based Hydrogen Storage Materials on the Properties of Composite Solid Propellant, *Chin. J. Energ. Mater.* **2009**, *17*, 501–504.
[10] H. Q. Sun, J. X. Zou, X. Q. Zeng, W. J. Ding, Synthesis and Hydrogen Storage Properties of Ultrafine Pure Mg and Mg-Nd Particles, *Rare Met. Mater. Eng.* **2012**, *41*, 1819–1823.
[11] J. E. Chen, Z. T. Xiong, G. T. Wu, Review on Hydrogen Storage in $Mg(BH_4)_2$, *J. Mater. Sci. Eng.* **2011**, *29*, 639–646.
[12] R. A. Varin, C. Chiu, Z. S. Wronski, Mechano-Chemical Activation Synthesis(MCAS) of Disordered $Mg(BH_4)_2$ using $NaBH_4$, *J. Alloys Compd.* **2008**, *462*, 201–208.
[13] J. Huot, G. Liang, S. Boily, A. V. Neste, R. Schulz, Structural Study and Hydrogen Sorption Kinetics of Ball-Milled Magnesium, *J. Alloys Compd.* **1999**, *293–295*, 495.
[14] H. Z. Liu, X. H. Wang, Y. G. Liu, Z. H. Dong, H. W. Ge, S. Q. Li, M. Yan, Hydrogen Desorption Properties of the MgH_2-AlH_3 Composites, *J. Phys. Chem. C* **2014**, *118*, 37–45.
[15] J. F. Stampfer, C. E. Holley, J. E. Shuttle, The Magnesium-Hydrogen System, *J. Am. Chem. Soc.* **1960**, *82*, 3504 – 3508.
[16] H. W. Li, K. Kikuchi, Y. Nakamori, N. Ohbab, K. Miwab, S. Towatab, S. Orimo, Dehydriding and Rehydriding Processes of Well-Crystallized $Mg(BH_4)_2$ Accompanying with Formation of Intermediate Compounds, *Acta Materialia* **2008**, *56*, 1342–1347.
[17] K. Chlopek, C. Frommen, A. Léon, O. Zabaraa, M. Fichtner, Synthesis and Properties of Magnesium Tetrahydroborate, $Mg(BH_4)_2$, *J. Mater. Chem.* **2007**, *17*, 3496–3503.
[18] T. Matsunaga, F. Buchter, P. Mauron, M. Bielman, Y. Nakamori, S. Orimo, N. Ohba, K. Miwa, S. Towata, A. Züttel, Hydrogen Storage Properties of $Mg(BH_4)_2$, *J. Alloys Compd.* **2008**, *459*, 583–588.
[19] D. I. Townsend, J. C. Tou, Thermal Hazard Evaluation by an Acceleration Rate Calorimeter, *Thermochim. Acta* **1980**, *37*, 1 – 30.
[20] T. B. Brill, K. J. James.Thermal Decomposition of Energetic Materials. 62. Reconciliation of the Kinetics and Mechanisms of TNT on the Time Scale from Microseconds to Hours, *J. Phys. Chem.* **1993**, *97*, 8759–8763.
[21] J. R. Hradel, *Enhanced Organic Explosives*, US Patent 3,012,868, Dow Chemical Corporation, Midland, MI, USA, **1961**.

Received: May 12, 2014
Revised: July 11, 2014
Published online: October 13, 2014

